Interactions of different types of localized corrosion in surgical implants

G. MORI*, H. DÖSINGER
Department of General and Analytical Chemistry, University of Leoben, Austria
E-mail: gregor.mori@notes.unileoben.ac.at

Surgical implants often show different types of localized corrosion such as corrosion fatigue cracking, pitting and crevice corrosion on the same part. Interactions of these different corrosion phenomena were investigated. This was done by cyclic loading of electropolished tensile specimens at different constant and changing potentials. Material investigated was a surgical implant steel X2CrNiMo18-15-3 which was immersed in physiological NaCl solution. Pitting and repassivation potentials were determined. Samples with and without artificial cracks as well as masked specimens were tested. Incubation period for first damage, density and size of pits by coulometric and volumetric method were determined. The fracture surfaces were then investigated by SEM.

Results show that not in all cases pitting corrosion was the cause for corrosion fatigue cracking. Also pitting is favoured by crack formation. Density of pits increases by a factor of 5 without any change to pitting potential. There are primary pits formed prior to crack initiation and secondary pits formed after crack initiation. At samples without crack there is almost no difference between the optically measured value of total pit volume and the coulometrically determined value. At samples with cracks coulometric volume of pits is much larger than optical one. This proves that there is a significant amount of crevice corrosion in the crack. The corrosion current density in the crack increases by two orders of magnitude when comparing it to electropolished surface of the sample. Results of laboratory experiments are confirmed by failure of a real implant.

1. Introduction

During the last three decades over 200 failed surgical implants have been investigated in cooperation with several hospitals and the Austrian Social Insurance for Occupational Risks. Reports on the causes of failure of implants are written approximately every 10 years [1–3]. Besides use of improper materials and insufficient constructions (e.g. too small cross sections, notches) fatigue cracking in conjunction with localized corrosion (pitting, crevice and fretting corrosion) is the most frequent cause for failures.

Generally cracks can be formed by forced fractures, stress corrosion cracking and fatigue or corrosion fatigue cracking. Forced fractures do not occur in surgical implants since bending of implant happens earlier. Stress corrosion cracking is also rather unlikely. This is due to the relatively low temperature in the human body. Consequently there are remaining two cracking mechanisms: fatigue and corrosion fatigue cracking. Distinction between both is often difficult, since in many cases there is only a small amount of corrosion present.

Corrosion fatigue can be initiated by constructive notches and by other corrosion mechanisms such as pitting. The latter yields from critical cyclic and/or constant stresses at the bottom of pits [4–13]. This interaction of corrosion and stresses is a well-known cause of failure, especially in stainless steels with their typically deep pits. On the other hand initiation of pits is favored by constant and cyclic stresses [14–17]. This means that stresses can also produce pits that will act as notches for crack formation. With concerns over this interaction one should not oversee that cracks can also produce crevice corrosion, while feigning pits are the primary cause of failure.

With respect to the effect of cracks on the initiation and formation of pits there are only very few works, that do not give a clear understanding of this relation [18, 19]. Therefore this work was done to find out possible interactions between different types of localised corrosion in surgical implants.

2. Experimental

Investigations with tensile specimens were carried out under static and dynamic loading. Equipment used was a

*Author to whom all correspondence should be addressed.

TABLE I Chemical composition of investigated steel X2CrNiMo18–15–3, material No. 1.4441, electropolished surface

Material No.	C (%)	Si (%)	Mn (%)	S (%)	P (%)	Cr (%)	Mo (%)	Ni (%)
1.4441	0.018	0.41	1.88	0.001	0.018	17.31	2.84	13.85

Rumul Mitron 654 pulser. Experiments were done under potentiostatic and potentiodynamic conditions. Samples were made of cold drawn surgical implant steel X2CrNiMo18–15–3, material No. 1.4441. Chemical composition and mechanical data of material is given in Tables I and II. Due to its low pitting resistance equivalent number (PREN = %Cr + 3%Mo) of 25.7 pitting formation in human body cannot be excluded with certainty [3]. Samples were electropolished with subsequent passivation in nitric acid. For the test solution deaerated physiological NaCl solution (0.9%) at 37 °C was used.

Before doing corrosion experiments with different potentials, fatigue and corrosion fatigue data of the investigating material have been determined. Table III summarizes results as a function of failure probability [20]. Sinusoidal cyclic stresses with a medium stress level of 580 MPa and amplitude of 280 MPa at a frequency of 50 Hz were used during corrosion fatigue tests. These values correspond to a failure probability in physiological NaCl solution of 95%. Pre-cracked specimens were prepared by applying cyclic stresses (580 $\pm$ 300 MPa) in distilled water.

Average pitting and repassivation potentials were determined by use of current density versus potential diagrams at a scan rate of 100 mV/h. Pit size, density and distribution was evaluated by an optical microscope and volumetric mass loss was determined from this data. Coulometric mass loss due to pitting was separately examined by integration of current–time-plots and current–potential-plots, respectively. Finally both mass loss values were critically compared. In addition fracture surfaces were examined by scanning electron microscopy (SEM).

3. Results

3.1. Potentiodynamic experiments

Mean values of pitting and repassivation potentials and corresponding standard deviations of three single measurements are presented in Table IV. Cyclic loading does not influence pitting potential in comparison to samples without external stresses. However for samples with an artificial crack generated by cyclic loading in distilled water the pitting potential was shifted by about 100 mV in the direction of more noble potentials.

Furthermore the slope of the current increase between pitting and reverse potential was about 40% higher for specimens not tested under stresses ($2.5 \cdot 10^{-7}\,A/cm^2/mV$) when compared to cyclic loaded samples ($1.5 \cdot 10^{-7}\,A/cm^2/mV$).

TABLE II Mechanical data of investigated steel X2CrNiMo18–15–3, material No. 1.4441, electropolished surface

Yield strength (MPa)	Tensile strength (MPa)	Elongation (%)	Reduction of area (%)
950	1220	15	59

The number of pits has been determined in three samples without mechanical stresses and with cyclic stresses respectively. Pit densities over the length of a sample are presented in Fig. 1 for both cases. There is an increase in the pit density in samples tested under cyclic loading by a factor of about 5. Also the effect of increasing pit density with increasing loads can be observed when comparing the number of pits in the thin center of the sample with that on the thicker edges.

3.2. Potentiostatic experiments

Specimens were tested for 12 h at a potential of 500 mV_{SHE}. This potential was chosen after determining the pitting potential, which is 70 mV nobler. However the pitting potential was determined potentiodynamically, which always results in slightly higher values. Consequently specimens with a potential of 500 mV_{SHE} are in the critical potential range for pitting and in fact showed a current increase due to pitting after 3–4 h of exposure time to the electrolyte. Electropolished samples without mechanical stresses and with no artificial crack showed after approximately 4 h an almost linear increase in current density per time with a slope, which is about $8.3 \cdot 10^{-6}\,A/cm^2/h$. Under cyclic loading incubation time for pitting formation was slightly reduced to 3.5 h. Current density per time increased to a rate of almost $1.2 \cdot 10^{-4}\,A/cm^2/h$, which is over 10 times higher than the value of non stressed specimens. In samples with an artificial crack no pits were generated within 12 h. This is due to the more noble pitting potential as mentioned earlier during potentiodynamic experiments.

3.3. Pit volume of potentiostatic and potentiodynamic experiments

Evaluation of the volume of pits has been measured by two methods. Firstly optical measurement was performed by determining the length, width and depth of

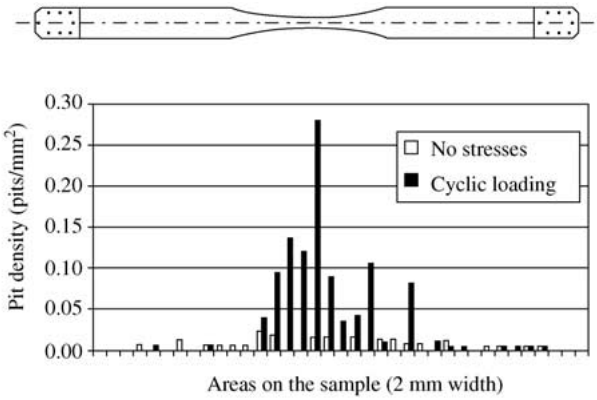

Figure 1 Pit density distribution on specimen tested without stresses and under cyclic stresses.

TABLE III Fatigue strength data of investigated steel X2CrNiMo18–15–3, material No. 1.4441, electropolished surface

Failure probability (%)	Fatigue strength	
	Air, 20 °C (MPa)	0.9% NaCl, 37 °C (MPa)
10	550	460
50	600	520
90	630	550
99	650	570

each pit under the assumption that the pits are cuboid in shape. In the case of crevice corrosion a typical pit depth for stainless steels was assumed according to a width to depth ratio of 1 [21]. This kind of calculation shows best results with respect to the irregular shape of many pits. Secondly a coulometric examination of the potentiostatic tests was done. Integration of the current versus time plot and use of the Faradaic law and the density of material yielded to the coulometrically determined pit volume in the specimens. Results are given in Figs. 2 and 3. There is a good agreement of pit volumes results determined by both methods in specimens without cracks. But results are contradicting in cracked samples, where the coulometric pit volume is much higher than the optical one. The smaller total pit volume of cracked samples in comparison to specimens without cracks is due to the longer duration of the latter experiments. Specimens were dismantled and cleaned after cracking. Specimens with no cracks remained in the test solution for a longer time.

Due to these results the charge density in cracks and crevices is expected to be higher than at the original sample surface. Therefore the difference between coulometric and volumetric pit volume was calculated for cracked samples as well as for specimens with an artificial crack. When dividing these values by the crack (or crevice) surface area one can find values for charge densities in this cracks and crevices, which can be compared with corresponding values of the original sample surface. Both the data for original sample surface and cracks (crevices) respectively are compared in Fig. 4. The charge density in cracks and crevices, respectively is about two orders of magnitude higher than at the sample surface. This result is independent of whether cracks are generated during or prior to the experiment or whether there is an artificial crevice.

TABLE IV Pitting and repassivation potentials determined from current density versus potential diagrams measured on specimens under different conditions

	No stresses		Cyclic loading no preliminary crack
	No preliminary crack	Preliminary crack generated in distilled water	
Pitting potential ($\mu \pm \sigma$) (mV_{SHE})	573 ± 59	680 ± 52	563 ± 23
Repassivation potential ($\mu \pm \sigma$) (mV_{SHE})	283 ± 15	300 ± 0	310 (1 value)

3.4. SEM investigations of fracture surfaces

Pits can clearly be divided into ''primary'' pits generated before crack initiation and ''secondary'' pits generated during crack propagation. Fig. 5(a) and (b) shows a part of the fracture surface with a pit that always represents a notch and served as a crack starter. Fracture paths lead from the pit radially in all directions of the fracture surface. The pit is located at the fracture origin and on both fracture surfaces of the fatigue crack.

In contradiction ''secondary'' pits as shown in Fig. 6(a) and (b) are located somewhere on the fracture surface but only on one of the two corresponding fractured parts. Most ''secondary'' pits are located near the sample surface so that these pits often reach the outer surface as shown in Fig. 6(a) and (b). A further result of fractographic investigations showed that ''secondary'' pits are generally larger than ''primary'' ones.

Pre-cracked samples with cracks initiated in distilled water show a fracture surface with deeper uniform corrosion attack than specimens with cracks generated in physiological NaCl solution at the bottom of a pit. In some pre-cracked specimens, large area fractions of the fracture surface were heavily corroded upto a depth of over 1 mm. An example with smaller uniform attack at the fracture surface is shown in Fig. 7. Between the arresting lines of the corrosion fatigue crack there is a significant mass loss due to crevice corrosion.

4. Discussion

Experiments show a five times higher pit density in samples with cyclic loading when compared with

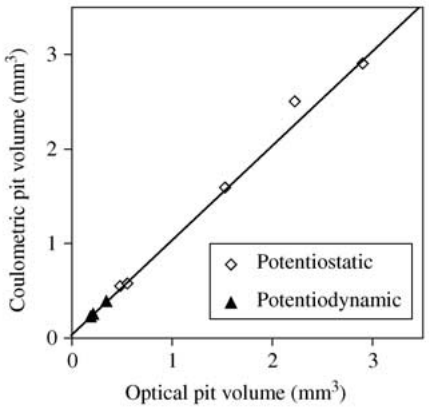

Figure 2 Comparison of coulometric and optical pit volume of specimens without crack tested under cyclic loading.

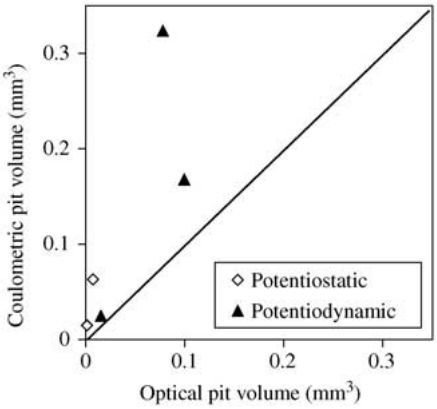

Figure 3 Comparison of coulometric and optical pit volume of specimens with crack tested under cyclic loading.

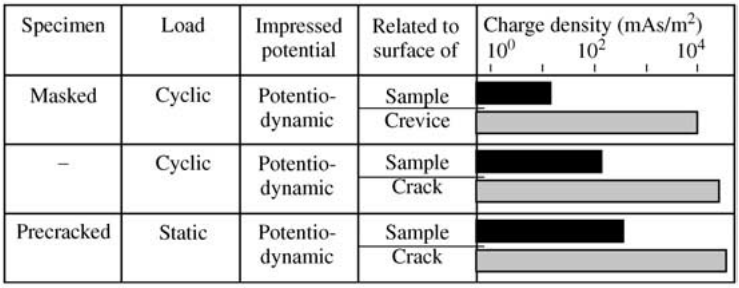

Figure 4 Charge densities on sample surface compared to that in cracks and crevices.

specimens without external stress level. The larger number of pits in these specimens is caused by formation of many local defects in the passive layer due to micro movements caused by alternating stresses. Detrimental effect of chloride ions to passive layer of stainless steel is supported by mechanical stresses yielding to a faster pit initiation. Cyclic loading does not influence pitting potentials. This was confirmed by potentiostatic and potentiodynamic experiments respectively, which is interesting because a direct relation between pit density and pitting potential could have been expected. Pitting potential was expected to be less noble during cyclic loading when compared to samples without external stresses. In pre-cracked samples pitting initiation is shifted to about 100 mV more noble potential, when compared to specimens without crack. This is due to further passivation during crack generation in distilled water.

Cyclic loaded specimens show a smaller slope of current density increase versus time than samples tested without cyclic loading. This can be explained by the vibration effects under cyclic stresses that retard formation of an aggressive electrolyte in pits.

Repassivation potentials are not influenced by cyclic stresses and pre-cracking. There was no vibration effect since all specimens failed before reaching repassivation potential. As a consequence in all samples an aggressive electrolyte could be formed in the pits.

The results show that not only does pitting favour corrosion fatigue crack initiation but also that cracking accelerates pit formation. There are ''primary'' pits formed prior to cracking and ''secondary'' pits generated

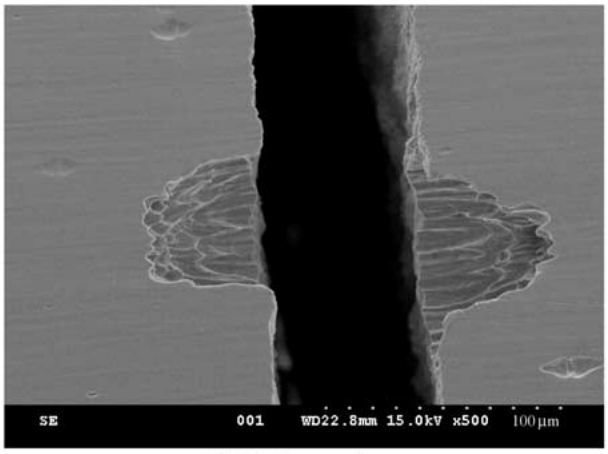

(a) Specimen surface

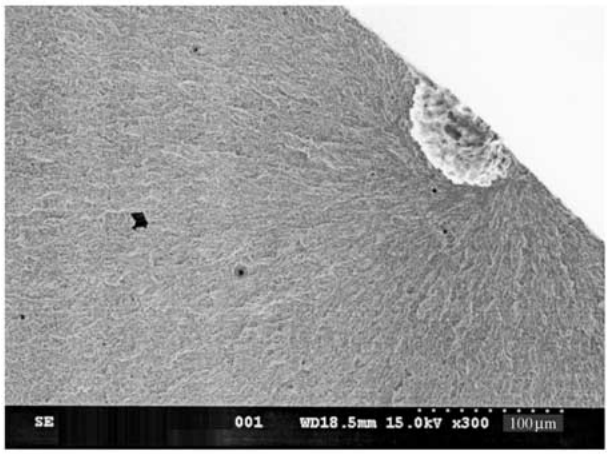

(b) Fracture surface

Figure 5 Primary pit as starter for corrosion fatigue cracking.

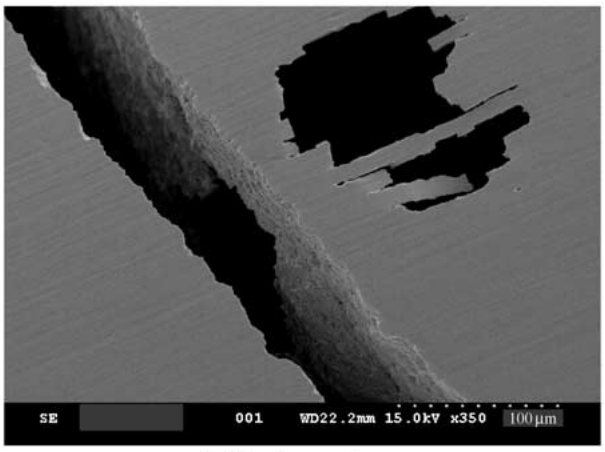

(a) Specimen surface

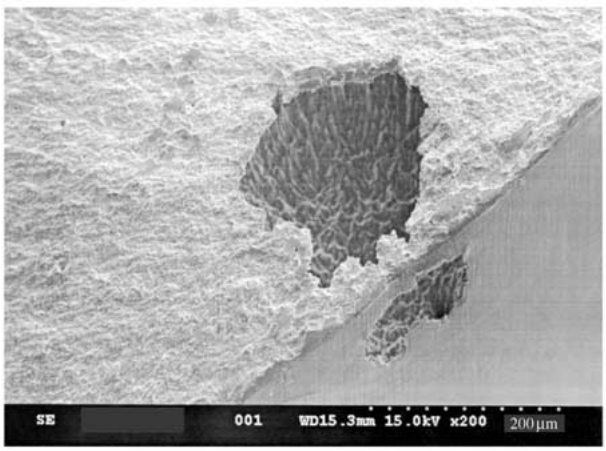

(b) Fracture surface

Figure 6 Secondary pit generated after crack initiation.

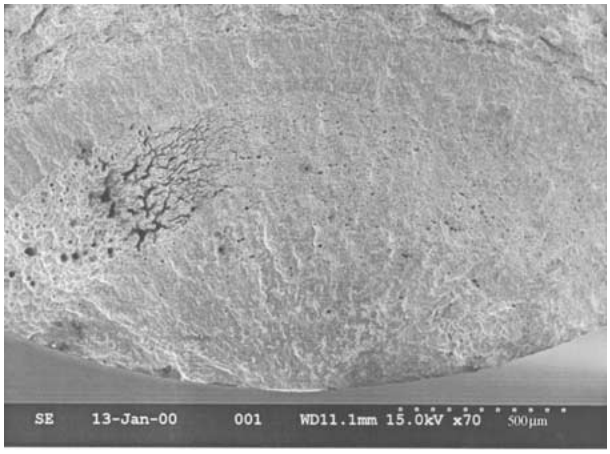

Figure 7 Crevice corrosion at fracture surface of pre-cracked specimen.

after crack initiation on the fracture surface. Distinction between both is clearly possible by fractography. ''Primary'' pits are located at the original sample surface or on both sides of the fracture surface. ''Secondary'' pits are located at the fracture surface and are only present on one of two fracture surfaces.

When looking at current density versus time plots, cyclic loaded specimens show a larger current density increase compared to samples tested without stresses. This is due to cracking of the samples. During cracking an active surface is generated which is more susceptible to corrosion attack. Additionally crevice corrosion forms in pre-cracked specimens.

In samples with cracks the ratio of coulometric pit volume is much larger than volumetric pit volume indicating a substantial amount of crevice corrosion in the crack. This assumption also has been proved by SEM investigation of fracture surfaces and by determination of charge density in the cracks and on the original surface of the specimens. All these results can be explained by the active surfaces that are formed during cracking and by crevice formation between fracture surfaces, respectively.

Fig. 8(a) and (b) show the surface and fracture surface of a surgical implant (Ender nail), which cracked after several month of service. On the surface of the part at the left side in Fig. 8(a) there seems to be a primary pit that may have served as the fracture origin. After investigating the fracture surface the primary pit turned out to be localized crevice corrosion (Fig. 8(b)). The fracture origin is located at one of the flutes at the surface of the part.

5. Conclusions

By means of potentiostatic and potentiodynamic experiments of electropolished austenitic stainless steel specimens with and without cyclic loading and with and without artificially pre-cracking, as well as crevices, the following results have been obtained:

- There is ''primary'' and ''secondary'' pit formation in cyclic loaded specimens. ''Primary'' pits gener-

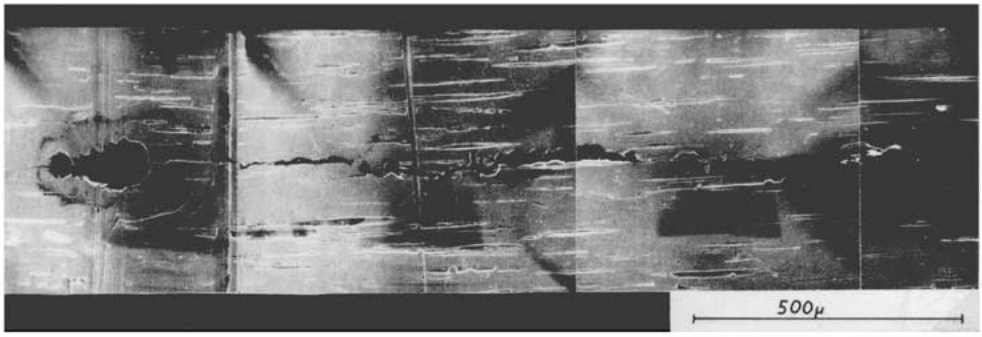

(a) Specimen surface

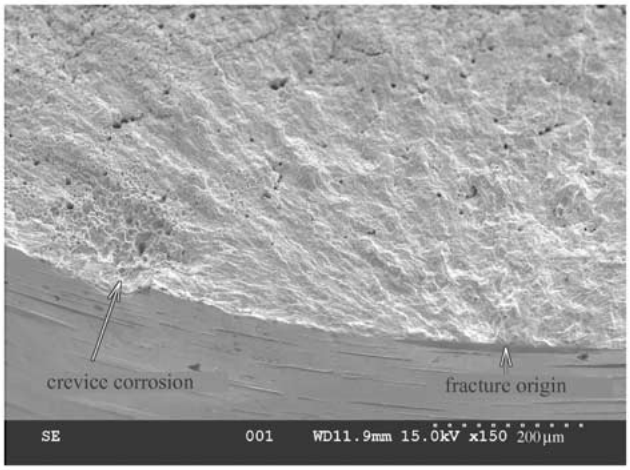

(b) Fracture surface

Figure 8 Corrosion fatigue cracking of a surgical implant with fracture origin at surface flute and crevice corrosion imitating a primary pit.

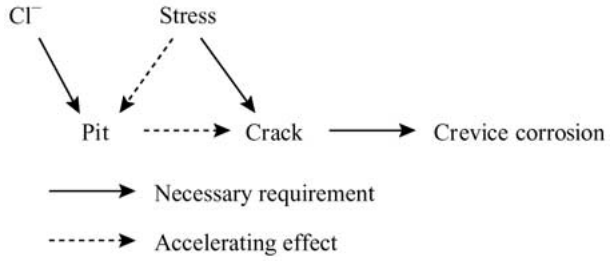

Figure 9 Possible interactions of localized corrosion, chloride ions and stresses.

ated before fatigue cracking serve as a notch and accelerate cracking of the samples. In contradiction cracks favor ''secondary'' pit formation when comparing samples with and without cracks. Distinction between ''primary'' and ''secondary'' pits is clearly possible by fractographic investigations.

- Vibration effects yield to a smaller increase of current density during pit formation when comparing samples tested with and without cyclic stresses retard formation of an aggressive electrolyte in pits during cyclic loading.
- Cyclic loading increases number of pits by a factor of five when compared to specimens under constant or no stresses. Pitting and repassivation potentials remain unaffected by this.
- Besides ''secondary'' pit formation in cracked samples there is a significant amount of crevice corrosion at the two fracture surfaces because of their active surface yielding to higher corrosion current densities at fracture surfaces and in crevices.

The following possible interactions of localized corrosion, chloride ions and stresses have to be considered (Fig. 9).

References

1. H. ZITTER, *Mater. Corr.* **22** (1971) 598.
2. H. ZITTER and D. SCHASCHL-OUTSCHAR, *ibid.* **32** (1981) 324.
3. H. ZITTER, *ibid.* **42** (1991) 455.
4. T. K. CHRISTMAN, *Corrosion* **46** (1990) 450.
5. S. R. NOVAK, in ''Proceedings of Corrosion Fatigue: Mechanics Metallurgy, Electrochemistry and Engineering, St. Louis, 1981'' (ASTM, Philadelphia, 1983) p. 26.
6. C. PATEL, V. ROLLINS and T. PYLE, *Nature* **266** (1977) 517.
7. R. EBRA and Y. YAMADA, in ''Proceeding of Corrosion Fatigue: Mechanics Metallurgy, Electrochemistry and Engineering, St. Louis, 1981'' (ASTM, Philadelphia, 1983) p. 135.
8. H. SPECKHARDT, in ''Proceeding of Corrosion Fatigue'' (NACE, Houston, Texas, 1972) p. 557.
9. S. J. LENNON, F. P. A. ROBINSON and G. G. GARRETT, *Corrosion* **40** (1984) 409.
10. S. SURESH, in ''Proceedings of Fatigue of Materials'' (Cambridge University Press, Cambridge, 1991) p. 120.
11. J. Q. WANG, J. LI, Z. F. WANG, Z. Y. ZHU, W. KE, Z. G. WANG and Q. S. ZANG, Script. *Metall. Mater.* **31** (1994) 1561.
12. K. KOMAI and K. MINOSHIMA, *Trans. Jap. Inst. Met.* **27** (1986) 23.
13. H. WIEGAND, H. SPECKHARDT and H. SPÄHN, *Stahl Eisen* **88** (1968) 726.
14. M. NAKAJIMA and K. TOKAJI, *Fatigue Fract. Eng. Mater. Struct.* **18** (1995) 345.
15. X. Y. ZHOU, D. L. CHEN, W. KE, Q. S. ZANG and Z. G. WANG, *Mater. Lett.* **7** (1989) 473.
16. J. WANG and J. LI, *Scr. Metall. Mater.* **29** (1993) 1415.
17. D. CHASTELL and P. DOIG, *Corr. Sci.* **19** (1979) 335.
18. J. I. DICKSON and L. SHIQIONG, *Mater. Charact.* **28** (1992) 327.
19. F. W. HIRTH, O. MICHEL and H. SPECKHARDT, *Werkst. Korr.* **23** (1972) 356.
20. H. WIESER, PhD thesis, University of Leoben, Austria (1997).
21. H. ZITTER, G. MORI, G. HOCHÖRTLER and H. WIESER, *Mater. Corr.* **53** (2002) 37.

Received 30 July 2002
and accepted 7 August 2003